Geochemical Perspectives Letters

© 2019 The Authors
Published by the European Association of Geochemistry

Graphite floatation on a magma ocean and the fate of carbon during core formation

H. Keppler, G. Golabek

Supplementary Information

The Supplementary Information includes:

- Methods
- Supplementary discussion
- Figure S-1
- Supplementary Information References

Methods

Calculation of the dynamic stability of graphite particles at the surface of a magma ocean

We studied the potential rise of graphite particles in a magma ocean following the method described in detail in Solomatov (2015). The convective heat flux q of the magma ocean can be calculated as

$$q = 0.089k\frac{(T_m - T_0)Ra^{1/3}}{D} \quad \text{(Eq. S-1)}$$

with the Rayleigh number

$$Ra = \left[\frac{\alpha_{Si} g \rho_{Si} (T_m - T_0) D^3}{\kappa \eta}\right] \quad \text{(Eq. S-2)}$$

and the thermal expansivity of the silicate melt α_{Si}, gravity acceleration $g = 4/3\pi\rho GR$, with silicate melt density $\rho_{Si} \approx 2700$ kg/m^3, G being Newton's constant, R the radius of the planetary object, potential temperature T_m , assumed surface temperature of space T_0 = 290 K, thermal diffusivity $\kappa = k/(\rho_{Si} c_P)$, thermal conductivity of silicates k, silicate melt heat capacity c_P and depth of the magma D. For the calculation of the gravity acceleration g close to the surface of each planetary object we use an average density $\rho = \rho_{Si} + (\rho_{Fe} - \rho_{Si})(D/R)^3$ assuming that each object is differentiated into an iron core with radius $R/2$ and density ρ_{Fe} and a magma ocean on top with silicate melt density ρ_{Si} and thickness $D = R/2$. At the rheological transition (melt fraction $\phi > 0.4$-0.6) the viscosity η in a magma ocean drops by orders of magnitude from $\eta \approx 10^{17}$ Pa s to $\approx 10^{-2}$ Pa s (Rubie *et al.*, 2003; Liebske *et al.*, 2005). The convective velocity in the magma ocean (Priestly, 1959; Kraichnan, 1962) is given as

$$v_S \approx 0.6\left(\frac{\alpha_{Si} g l q}{\rho_{Si} c_P}\right)^{1/3} \quad \text{(Eq. S-3)}$$

with mixing length $l \approx D \approx R/2$.

We used the results of two laboratory experiments to estimate the size of graphite particles that can be suspended by convective flow. Based on Shraiman and Siggia (1990) the largest entrained graphite particles have a diameter given as

$$d \leq \frac{\rho_{Si}\left(\frac{v_S}{x^*}\right)^2}{0.1\left(\rho_{Si} - \rho_G\right) g} \quad \text{(Eq. S-4)}$$

with graphite density $\rho_G \approx 2250$ kg/m^3 and constant factor $x^* = 60$. Using the results by Solomatov *et al.* (1993) we obtain the following equation for the diameter of the largest entrained graphite particles

$$d \leq \frac{\left(\frac{\eta_l \alpha_{Si} q}{c_P}\right)^{1/2}}{0.1\left(\rho_{Si} - \rho_G\right) g^{1/2}} \quad \text{(Eq. S-5)}$$

where η_l is the viscosity of silicate melt set to 10^{-2} Pa s (Rubie *et al.*, 2003; Liebske *et al.*, 2005).

Thermodynamic calculation of carbon solubility in a magma ocean in equilibrium with graphite

The fugacities of CO and CO_2 in equilibrium with graphite are controlled by the two equilibria

$$C + ½\ O_2 = CO \quad \text{(Eq. S-6)}$$

$$C + O_2 = CO_2 \quad \text{(Eq. S-7)}$$

Obviously, if the oxygen fugacity is imposed by the oxidation state of the magma ocean, the fugacities of both CO and CO_2 are fixed at a given temperature and can be readily calculated using the thermodynamic data for CO and CO_2 tabulated in Robie and Hemingway (1995). The oxygen fugacity of the IW (Fe-FeO buffer; Fig. 1) was calculated from the thermodynamic data of FeO in Robie and Hemingway (1995).

The solubilities of CO and CO_2 in a silicate melt follow Henry´s law, i.e. the dissolved concentrations c of CO and CO_2 are directly proportional to their fugacity in the gas phase. Therefore

$$cc^{melt} = K_{CO}\, f_{CO} + K_{CO2}\, f_{CO2} \quad \text{(Eq. S-8)}$$

where K_{CO} and K_{CO2} are the Henry constants of CO and CO_2, respectively, expressed as ppm carbon per bar, and f_{CO} and f_{CO2} are the fugacities of CO and CO_2. The solubility of CO_2 in silicate melts may be described by $K_{CO2} = 0.155$ ppm C/bar for a wide range of compositions (Ni and Keppler 2013). Yoshioka *et al.* (2019) found that the CO solubility in MORB melt may be described by the equation $\log c_{CO} = -5.20 + 0.80 \log f_{CO}$ ($R^2 = 0.83$) with c_{CO} being expressed as carbon in wt. %. Since the coefficient in front of the log f_{CO} term is close to 1, at low pressures this relationship may also be approximately described by a Henry constant of $K_{CO} = 0.016$ ppm C/bar. While this Henry constant is based on experiments with MORB melt, the study of Yoshioka *et al.* (2019) suggests that the solubility is not very dependent on melt composition and therefore, the same solubility law may be used as a reasonable approximation for a peridotite melt. With these assumptions, the carbon solubilities in Figure 2 were calculated from equation S-8.

Calculation of carbon extraction from the magma ocean during core formation

The maximum carbon concentration that may be reached in the core of a growing planet, if the accreted metal only extracts the carbon present in the silicate melt phase of the magma ocean can be easily calculated. We assume that the accretion of a planet with final mass M occurs in N equal steps; i.e. there are N impact events, which cause the planet to grow. This means that the mass m_m of metal added during each step is

$$m_m = \frac{Mf}{N} \quad \text{(Eq. S-9)}$$

where f is the fraction of metal in the impactor, which we assume to be constant. The metal added rapidly sinks to the core; after reaching the core, there is no further equilibration, as assumed in all current models of core formation (e.g. Rubie *et al.* 2011, 2015).

The mass of the silicate melt m_s in a deep magma ocean extending down to the mantle core boundary after the nth impact event is then

$$m_s = \frac{nM(1-f)}{N} \quad \text{(Eq. S-10)}$$

The equilibrium concentration of carbon in the silicate melt, as adjusted by the equilibrium with graphite and the gas phase on the surface is c_s; due to the very high metal/silicate partition coefficients of carbon under reducing conditions (see Fig. 3b), one may assume in good approximation that almost all of the carbon originally present in the melt is sequestered by the metal phase, yielding the carbon concentration in the metal c_m for the nth impact

$$c_m = c_s \frac{m_s}{m_m} = c_s n \frac{1-f}{f} \quad \text{(Eq. S-11)}$$

The average carbon concentration in the core after complete accretion is then

$$\overline{c_m} = \frac{1}{N}\sum_{n=1}^{N} c_s n \frac{1-f}{f} = c_s (N+1)\frac{1-f}{2f} \quad \text{(Eq. S-12)}$$

Discussion

Carbon solubility in a magma ocean in the presence of methane

The model calculations for the behavior of carbon in a magma ocean as outlined in this study are based on the simple C-O system, where the fugacities are controlled by the equilibrium of the gas phase with graphite and the magma ocean. These fugacities will not change if other volatile components are present. However, in the presence of water or hydrogen, some methane may form as additional species, which may contribute to bulk carbon solubility. According to the equilibrium

$$C + 2\,H_2 = CH_4 \quad \text{(Eq. S-13)}$$

the fugacity of methane in equilibrium with graphite is controlled by the fugacity of hydrogen (H_2). In Figure S-1a, we calculated methane fugacity for a range of temperatures and H_2 fugacities from 1 to 1000 bar, using the thermodynamic data from Robie and Hemingway (1995). The diagram shows that in order to stabilize appreciable amounts of CH_4, very high hydrogen fugacities are required. This is due to the fact that the Gibbs free energy of formation of methane at high temperature is distinctly positive.

The solubility of methane in a basaltic melt at 1400 °C was studied by Ardia *et al.* (2013). At low pressures, their data suggest a Henry constant for methane of 138.4 ppm C/GPa, which equals 0.0138 ppm C per bar of CH_4 partial pressure. This number is

actually rather similar to that for CO (see above). If one assumes that the solubility data of Ardia *et al.* (2013) may also be applied to a peridotitic melt and neglects a possible temperature dependence, the solubility of methane in a magma ocean may be calculated, as shown in Figure S-1b. The contribution of methane to bulk carbon solubility is very low, below 1 ppm for hydrogen fugacities up to several 100 bar. Such high hydrogen fugacities are, however, implausible for magma ocean temperatures. At a temperature of 2000 K, the average velocity v of a H_2 molecule would be 4.1 km/s, according to the relationship $1/2\ mv^2 = kT$, where k is the Boltzmann constant and m is the mass of H_2. This value is close to the planetary escape velocity for smaller planets such as Mercury (4.2 km/s), but below that for Earth (11.2 km/s). Since there is a statistical distribution of molecular velocities, a significant fraction of H_2 molecules will reach velocities even above the terrestrial escape velocity, such that even for an Earth-size planet, rapid loss of hydrogen to space will occur (e.g. Volkov *et al.* 2011). We therefore conclude that the contribution of methane to bulk carbon solubility in a magma ocean can be ignored under all plausible circumstances.

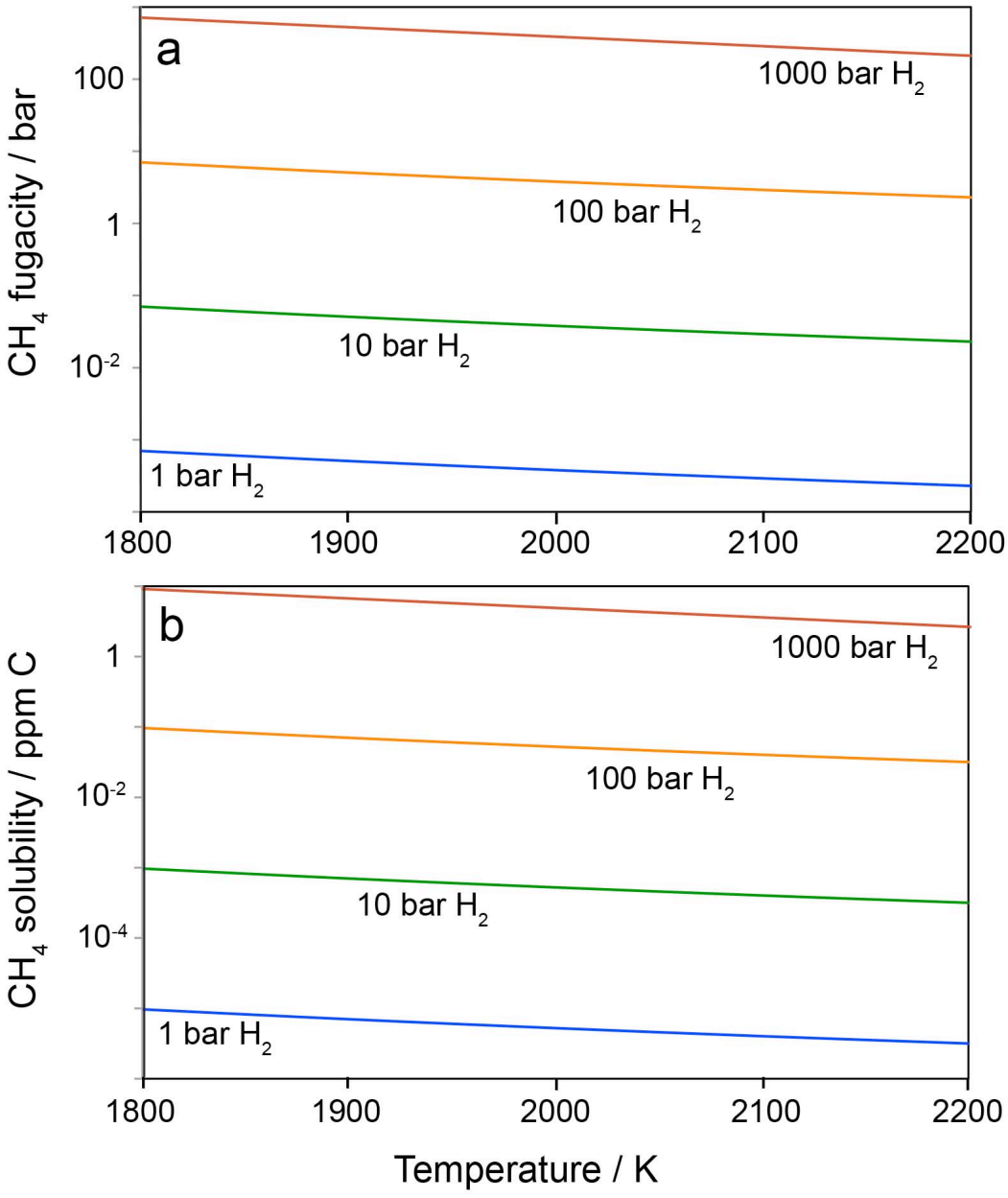

Figure S-1 Methane (CH_4) fugacity (a) and methane solubility in a magma ocean (b) for H_2 fugacities from 1 to 1000 bar and temperatures from 1800 to 2200 K

Possible graphite floatation and formation of a graphite-rich crust on Mercury

Due to its highly reducing nature, planet Mercury may provide a good example for the process of graphite floatation. Namur *et al.* (2016) compared the sulfur concentration in lavas on the surface of Mercury with experimentally determined sulfur solubilities in silicate melts and concluded that they record a log fO_2 of IW-5.4. Somewhat less reducing conditions may be inferred from the low FeO content of the corresponding magmas, with log fO_2 ranging from IW-2.8 to IW-4.5 (Cartier and Wood 2019). At these low oxygen fugacities, our models predict that a large fraction of the total carbon in the planet should precipitate as graphite, rather than being sequestered into the core (Fig. 4 of main text) and floatation of this graphite on the surface of the magma ocean is plausible (Fig. 2 of main text), in particular, if one allows for some sintering of graphite into larger aggregates. This is entirely consistent with the direct detection of a graphite-rich crust on the surface of Mercury by remote-sensing techniques (Peplowski *et al.* 2016).

The possibility of graphite floating on the surface of a Mercurian magma ocean was already raised by van der Kaden and McCubbin (2015) based on simple density arguments. However, they did not investigate the dynamic stability of graphite in a convecting magma ocean, nor did they provide a thermodynamic reason for abundant graphite precipitation. Cartier and Wood (2019) suggested that the carbon enrichment on the surface of Mercury may be due to carbon becoming more lithophile at very reducing conditions. It should be noted that the mechanism in the model presented here is very different. As shown in Figure 3 (main text) and following the model of Chi *et al*. (2014) $D_C^{metal/silicate}$ actually increases continuously under more reducing conditions. The inefficient segregation of carbon into the core is in our model caused by the very low carbon solubility in the silicate melt in equilibrium with floating graphite. The near constancy of the carbon content in metal coexisting with graphite (Fig. 3b, main text) provides an independent thermodynamic test that verifies the assumptions in our model.

The importance of graphite relative to diamond in sequestering carbon from a magma ocean.

Hirschmann (2012) proposed that diamond may precipitate from a magma ocean at greater depth; the diamond may then sink until it remains neutrally buoyant in the magma ocean. In this way, a carbon-enriched layer could be produced in the mantle. While such a process may be conceivable, we consider it to be unlikely for two reasons. (1) The difference in Gibbs free energy between graphite and diamond is small at upper mantle conditions. At given oxygen fugacity, the solubility of solid carbon (graphite or diamond) will therefore be primarily controlled by temperature und pressure. At graphite or diamond saturation, carbon solubility in the melt probably gently decreases with pressure (e.g. Eguchi and Dasgupta 2018), but increases with temperature (see Fig. 3 of the main text). Since the temperature at the surface of the magma ocean is expected to be much lower than deep in its interior, the surface is the most plausible place for carbon precipitation in the form of graphite. Moreover, most of the carbon will be delivered from the beginning as graphite-like material, which is likely dynamically stable on the magma ocean surface (Fig. 2 of the main text). (2) Due to the vanishing density difference between diamond and peridotite melt at the depth of neutral buoyancy, it would likely be re-entrained into the convective currents of the magma ocean, thus no carbon-enriched layer could form.

Supplementary Information References

Ardia, P., Hirschmann, M.M., Withers, A.C., Stanley, B.D. (2013) Solubility of CH_4 in a synthetic basaltic melt, with applications to atmosphere–magma ocean–core partitioning of volatiles and to the evolution of the Martian atmosphere. *Geochimica et Cosmochimica Acta* 114, 52–71

Cartier, C., Wood, B.J. (2019) The role of reducing conditions in building Mercury. *Elements* 15, 39-45.

Eguchi, J., Dasgupta, R. (2018) A CO_2 solubility model for silicate melts from fluid saturation to graphite or diamond saturation. *Chemical Geology* 487, 23–38.

Hirschmann, M.M. (2012) Magma ocean influence on early atmosphere mass and composition. *Earth and Planetary Science Letters* 341-344, 48–57.

Kraichnan, R.H. (1962) Turbulent thermal convection at arbitrary Prandtl number. *Physics of Fluids* 5, 1374–1389.

Liebske, C., Schmickler, B., Terasaki, H., Poe, B.T., Suzuki, A., Funakoshi, K.-I., Ando, R., Rubie, D.C. (2005). Viscosity of peridotite liquid up to 13 GPa: Implications for magma ocean viscosities. *Earth and Planetary Science Letters* 240, 589–604.

Namur, O., Charlier, B., Holtz, F., Cartier, C., Mccammon, C (2016) Sulfur solubility in reduced mafic silicate melts: Implications for the speciation and distribution of sulfur on Mercury. *Earth and Planetary Science Letters* 448, 102-114.

Ni H., Keppler H. (2013) Carbon in silicate melts. *Reviews in Mineralogy and Geochemistry* 75, 251-287.

Priestly, C.H.B. (1959) *Turbulent Transfer in the Lower Atmosphere*. University of Chicago Press, Chicago, IL.

Robie, R.A., Hemingway, B.S. (1995) Thermodynamic Properties of Minerals and Related Substances at 298.15 K and 1 Bar (10^5 Pascals) Pressure and at Higher Temperatures. *US Geological Survey Bulletin* 2131.

Rubie, D.C., Melosh, H.J., Reid, J.E., Liebske, C., Righter, K. (2003) Mechanisms of metal-silicate equilibration in the terrestrial magma ocean. *Earth and Planetary Science Letters* 205, 239-255.

Solomatov, V.S. (2015). Magma oceans and primordial mantle differentiation. In: *Treatise on Geophysics* Vol. 9, 81–104.

Van Der Kaaden, K. E., Mccubbin, F. M. (2015) Exotic crust formation on Mercury: consequences of a shallow, FeO-poor mantle. *Journal of Geophysical Research* 120, 195-209.

Volkov, A., Johnson, R.E.Tucker, O.J., Erwin, J.T. (2011) Thermally driven atmospheric escape: transition from hydrodynamic to jeans escape. *The Astrophysical Journal Letters* 729, L24.

Yoshioka, T., Nakashima, D., Nakamura, T., Shcheka, S., Keppler, H. (2019) Carbon solubility in silicate melts in equilibrium with a CO-CO_2 gas phase and graphite. *Geochimica et Cosmochimica Acta* 259, 129-143.